JOURNAL OF SOLID STATE CHEMISTRY 9, 279–296 (1974)

The Physical Properties of Linear Chain Systems
I. The Optical Spectra of $[(CH_3)_4N]NiCl_3$, $Cs(Mg,Ni)Cl_3$, $CsNiCl_3$, $RbNiCl_3$ and $CsNiBr_3$*

J. ACKERMAN, E. M. HOLT, AND S. L. HOLT

The Department of Chemistry, University of Wyoming, Laramie, Wyoming 82070

Received March 21, 1973

The single crystal spectra of pure $CsNiCl_3$, $CsNiBr_3$, $RbNiCl_3$, and $[(CH_3)_4]NiCl_3$, and the single crystal spectrum of $CsNiCl_3$ diluted in $CsMgCl_3$ have been measured to 5°K. The spectra of the magnetically concentrated materials show a number of anomalously intense maxima. These are interpreted in terms of cooperative interactions.

Introduction

A major area of interest in our laboratories has centered around the elucidation of the electronic structures of first row transition metal ions. These investigations have dealt with ions in high oxidation states (*1*), ions in trigonal and lower symmetry environments (*2*), and ions in cubic host lattices (*3*). Our more recent efforts have been directed toward the elucidation of the physical properties of compounds in which the metal ions are antiferromagnetically coupled. These studies have involved species such as $LiCrO_2$ (*4*) and $NiCl_2$ (*5*), which are coupled in three dimensions [3] and those in which the coupling is primarily in one dimension [1] only (*6–8*).

Measurements of the magnetic susceptibility (*6*) and neutron diffraction spectrum (*7, 8*) of $[(CH_3)_4N]MnCl_3$ (TMMC) have shown that it is a [1] linear chain antiferromagnet to 0.84°K. This behavior differs somewhat from that reported for the members of the group $M^IM^{II}X_3$ ($M^I = Rb^+$ or Cs^+; $M^{II} = Ti^{2+}$, V^{2+}, Cr^{2+}, Fe^{2+}, Co^{2+}, Ni^{2+}, or Cu^{2+}; $X = Cl^-$ or Br^-) (*9*) even though these latter compounds possess structures quite similar to TMMC. This structure consists of parallel linear chains of face sharing $M^{II}Cl_6$ octahedra (*10, 11*) separated by the M^I cations. For TMMC the $(CH_3)_4N^+$ cation is sufficiently bulky to provide complete magnetic insulation between adjacent chains. For the compounds containing the less bulky Rb^+ and Cs^+ cations, the magnetic insulation is less complete, allowing [3] order to set in in some instances at temperatures considerably in excess of 4°K.

Optical spectroscopy has played an important role in the study of exchange coupled systems (*12*). In such systems it has been found that well-defined spin–wave excitations exist for temperatures up to and, in certain cases, beyond T_N (*7, 8, 13–15*). This phenomenon is of importance optically because of the manifestation of spin–wave (magnon) side bands under suitable conditions. These magnon side bands occur when two neighboring magnetic ions undergo a simultaneous transition. One of the ions undergoes a normal *d–d* or *f–f* transition while the second ion undergoes a spin deviation such that the total spin is conserved. This leads to the observation of relatively sharp maxima which are not observed in magnetically dilute systems. While such transitions have been studied in detail for two and three dimensional systems, little is known about the optical manifestation of magnons for systems in which the spin correlation is one dimensional [1]. Dingle et al. (*6*) have investigated the optical properties of TMMC to 1.2°K without observing magnon side bands even though it has been shown that short range spin correlations exist in TMMC at

* Supported by NSF Grant No. 15432 A1, the Office of Naval Research, and the Research Corporation.

temperatures significantly above T_N (*7*, *8*). It is uncertain as to whether this absence of magnon side bands is due to the [1] nature of the spin correlations in TMMC or merely the result of measurements being made at temperatures too much in excess of T_N for the phenomena of spin–wave side bands to be observed.

In an attempt to ascertain the relative importance of interchain vs intrachain interactions and to elucidate the electronic structure of some magnetically coupled Ni^{2+} systems, we have measured the absorption spectra of $[(CH_3)_4N]NiCl_3$, $RbNiCl_3$, $CsNiCl_3$, $CsNiBr_3$, and $Cs(Ni,Mg)Cl_3$ to 5°K.

Asmussen and Solig (*16*), Day (*17*), Hatfield and Piper (*18*), Goodgame et al. (*19*), and McPherson and Stucky (*20*) have conducted the only previous studies of the optical properties of $CsNiCl_3$, $CsNiBr_3$, $RbNiCl_3$, and $[(CH_3)_4N]$-$NiCl_3$. These measurements, however, were made either on polycrystalline samples or at temperatures considerably in excess of those at which our measurements have been made and do not reveal many of the features which we report here.

Crystal Structures

$CsNiCl_3$ and $RbNiCl_3$ are isomorphous with $CsMgCl_3$ (*10*, *11*). All three of these compounds belong to space group $P6_3/mmc$ with $CsNiCl_3$ and $RbNiCl_3$ having cell dimensions (*11*) of $a =$ 7.18 Å, $c = 5.93$ Å and $a = 6.95$ Å, $c = 5.90$ Å, respectively, and $CsMgCl_3$ displaying the dimensions (*10*) $a = 7.269 \pm 0.006$ Å, $c = 6.187 \pm 0.005$ Å. The principal structural feature consists of parallel linear arrays of face sharing $[MCl_6]$ octahedra. The M^{2+} ion lies on a site of D_{3d} symmetry.

The $[(CH_3)_4N]NiCl_3$ compound possesses a similar linear chain structure but belongs to space group $P6_3/m$ or $P6_3$ (*21*). The cell dimensions are $a = 9.019$ and $c = 6.109$ Å.

Experimental

Single crystals of $CsNiCl_3$ were prepared by mixing equimolar ratios of reagent grade CsCl and $NiCl_2$ (made by dehydrating $NiCl_2 \cdot 6H_2O$ at 110°C in a stream of HCl gas), placing the mixture in an evacuated quartz ampoule, and zone refining it. Single crystals of $CsNiBr_3$, $RbNiCl_3$, and of $CsMgCl_3$ containing small amounts of Ni^{2+} were prepared in the same way. Single crystals of $[(CH_3)_4N]NiCl_3$ were prepared by slow evaporation of an equimolar mixture of $[(CH_3)_4N]Cl$ and $NiCl_2 \cdot 6H_2O$ which were mixed in 10% HCl, 90% H_2O.

Crystals suitable for σ and π optical measurements were cleaved parallel to the c crystallographic axis, polished where necessary, and checked for proper alignment using Weissenberg and precession photography.

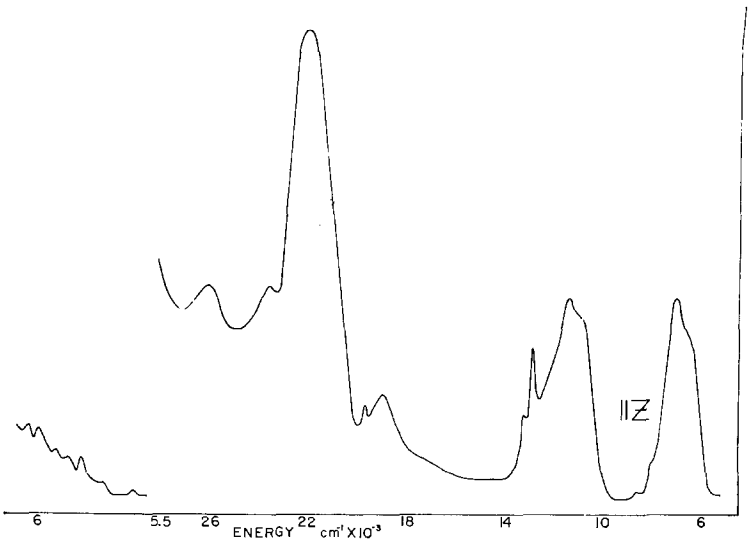

FIG. 1. The 5°K spectrum of $[(CH_3)_4N]NiCl_3$, $\|Z$.

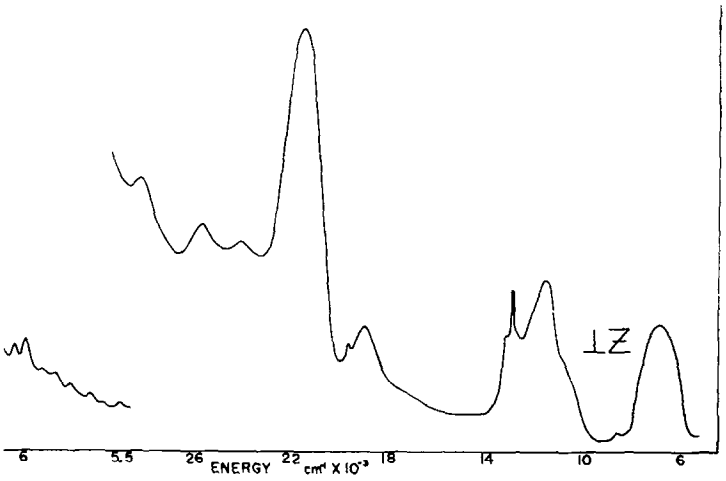

FIG. 2. The 5°K spectrum of $[(CH_3)_4N][NiCl_3$, $\perp Z$.

Optical measurements were made at 300, 80, and 5°K with a Cary 14R recording spectrophotometer using techniques previously described (*1*, *2*).

Great difficulty was encountered while attempting to prepare crystals suitable for optical measurements with the direction of the propagation along the unique axis as the material tends to spontaneously cleave parallel to the *c* axis. After numerous attempts it was found possible by careful polishing, to obtain crystals suitable for axial spectra.

Results

The polarized spectra of $[(CH_3)_4N]NiCl_3$, $Cs(Mg,Ni)Cl_3$, $CsNiCl_3$, $RbNiCl_3$, and $CsNiBr_3$ taken at 5°K are shown in Figs. 1–9. Figures 10–15 display the temperature dependence of the absorption spectra of $CsNiCl_3$, $RbNiCl_3$, and $CsNiBr_3$ in the 5000–20000 cm^{-1} region. Tables I–V contain a tabulation of the energies of the various components of the absorption manifolds and their assignments. In Table VI may be found the best-fit calculated energies

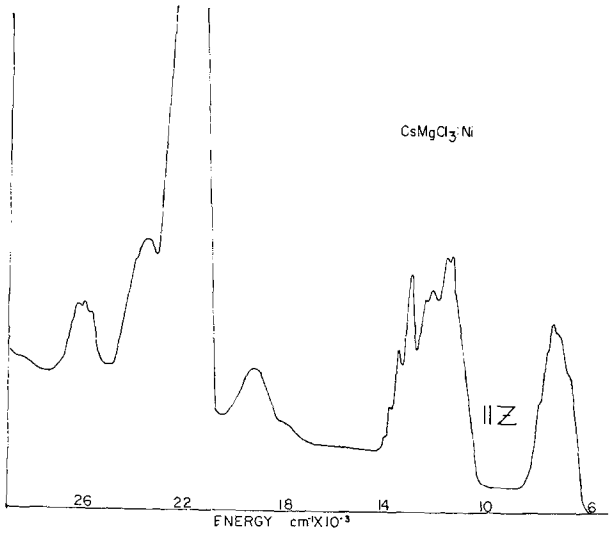

FIG. 3. The 5°K spectrum of $CsMgCl_3$:Ni, $\|Z$.

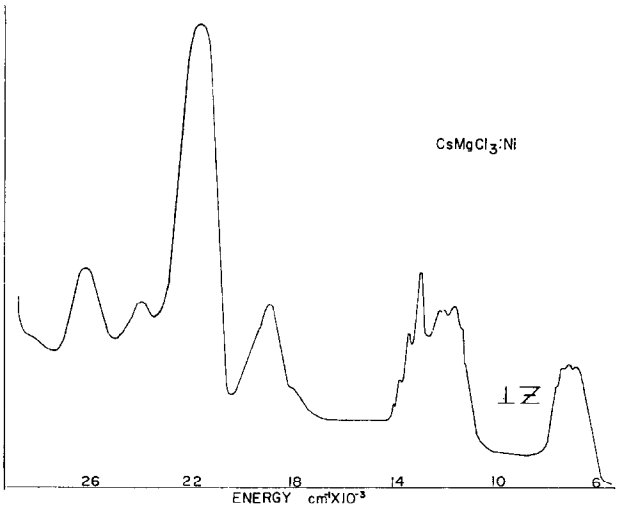

FIG. 4. The 5°K spectrum of $CsMgCl_3$:Ni, $\perp Z$.

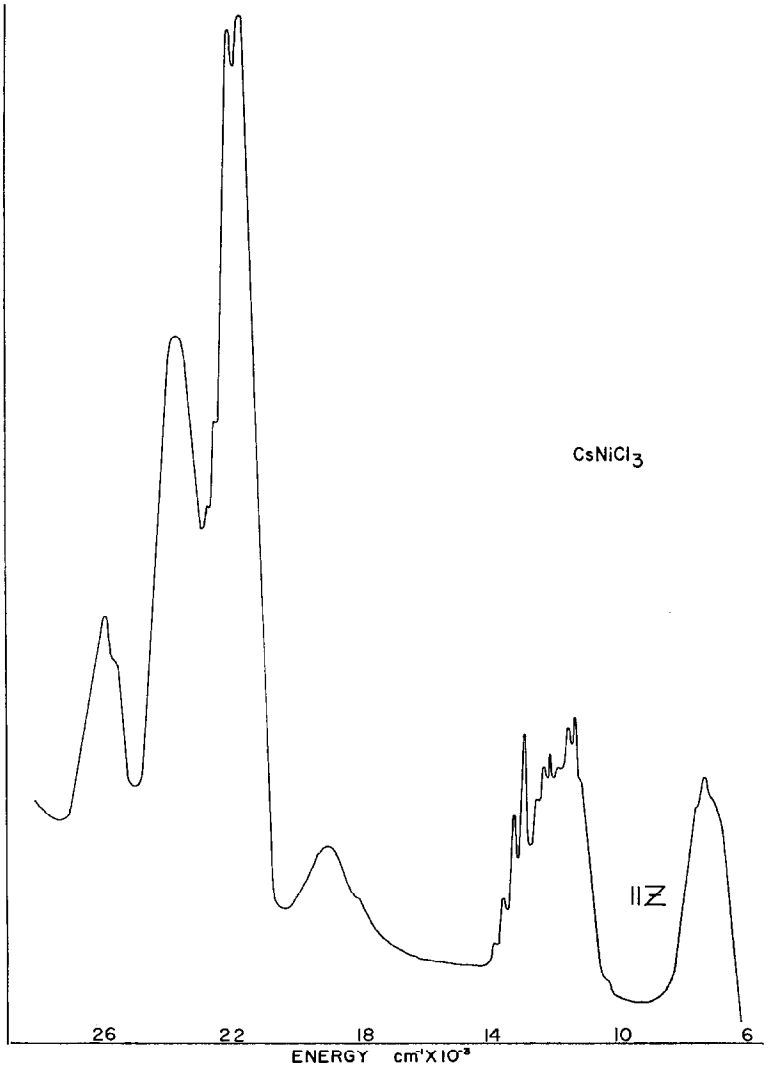

FIG. 5. The 5°K spectrum of $CsNiCl_3$, $\|Z$.

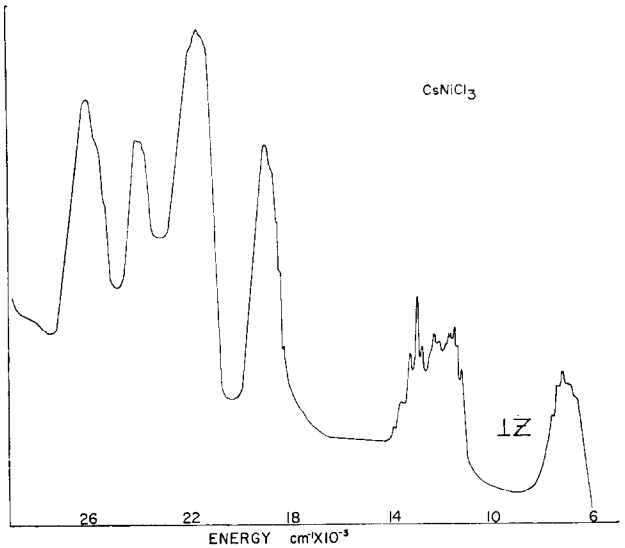

FIG. 6. The 5°K spectrum of $CsNiCl_3$, $\perp Z$.

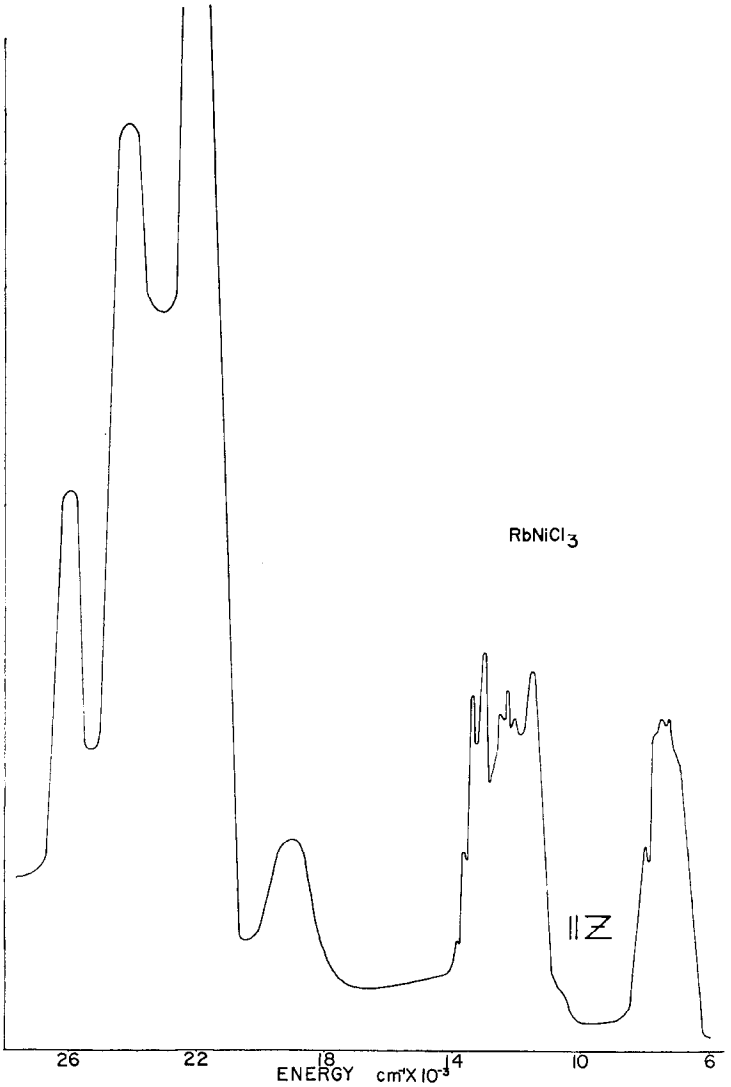

FIG. 7. The 5°K spectrum of $RbNiCl_3$, $\|Z$.

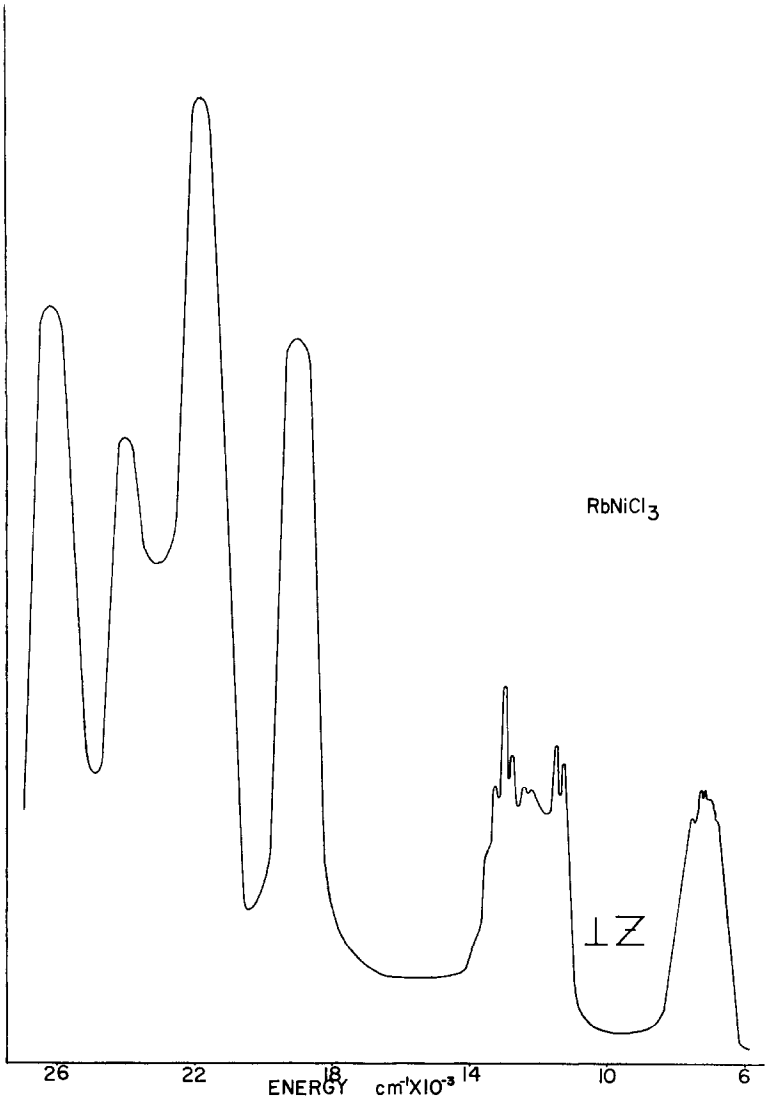

FIG. 8. The 5°K spectrum of $RbNiCl_3$, $\perp Z$.

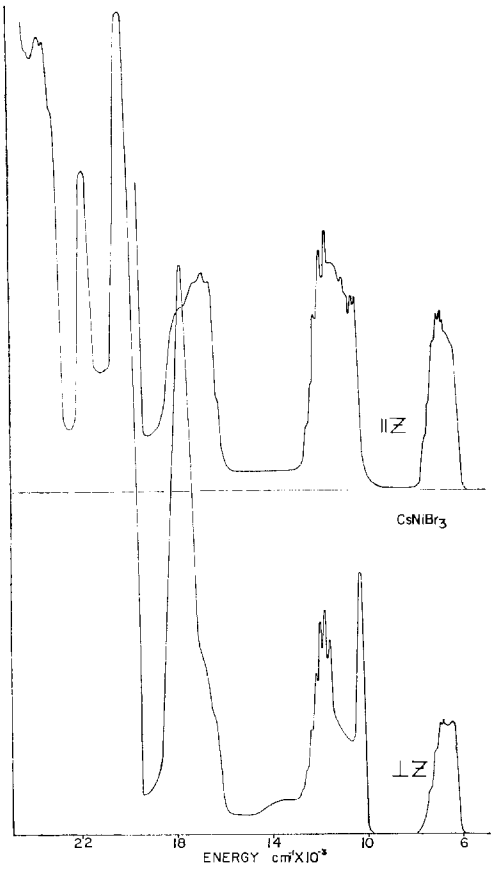

FIG. 9. The 5°K spectrum of $CsNiBr_3$.

FIG. 10. The temperature dependence of the spectrum of $CsNiCl_3$, $\|Z$.

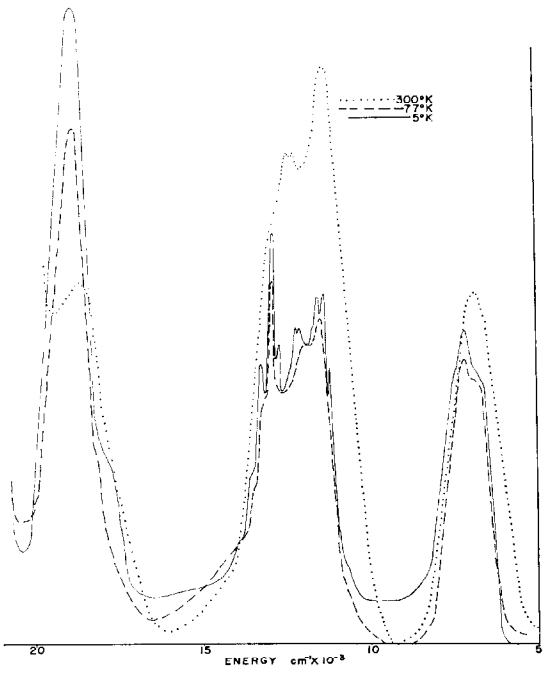

FIG. 11. The temperature dependence of the spectrum of $CsNiCl_3$, $\perp Z$.

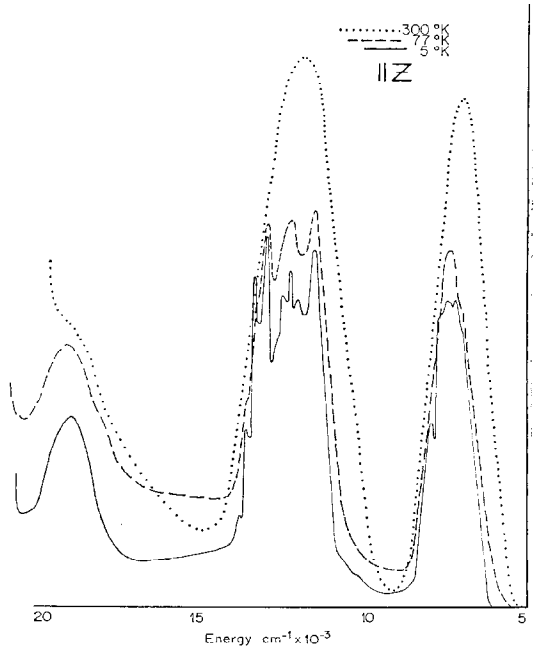

FIG. 12. The temperature dependence of the spectrum of $RbNiCl_3$, $\|Z$.

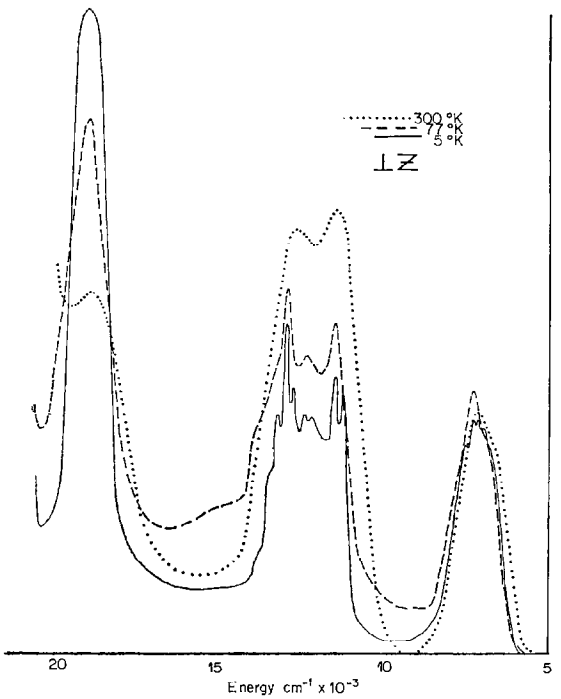

FIG. 13. The temperature dependence of the spectrum of $RbNiCl_3$, $\perp Z$.

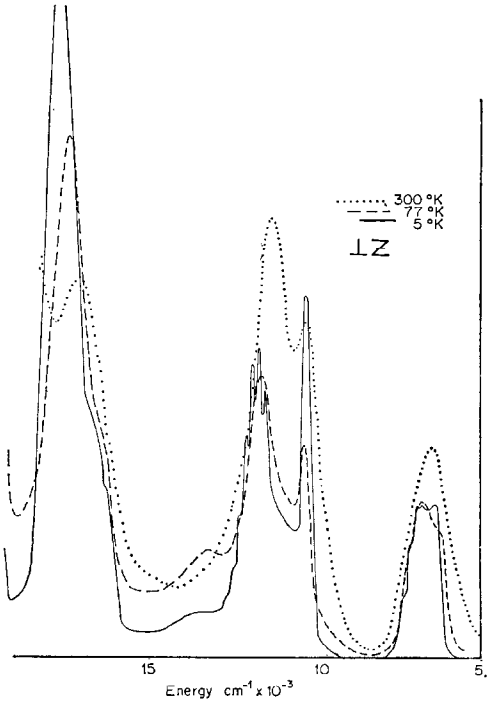

FIG. 15. The temperature dependence of the spectrum of $CsNiBr_3$, $\perp Z$.

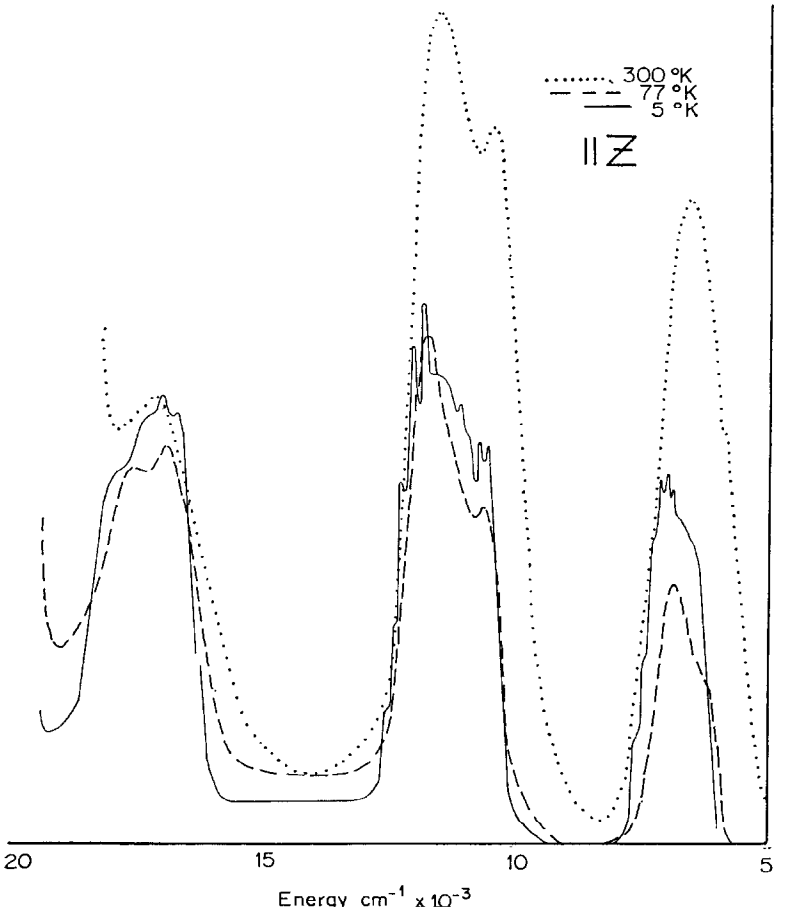

TABLE I

THE ABSORPTION SPECTRUM OF $Cs(Mg,Ni)Cl_3$ AT 5°K

E, cm^{-1}	ΔE	Assignment
		$E\|\|z$
6623		$^3A_{2g} \rightarrow {}^3A_{2g}$ [a]
7380		$^3A_{2g} \rightarrow {}^3E_g + 1E_{1u}^{A1}$ [b]
	225	
7605		$^3A_{2g} \rightarrow {}^3E_g + 2E_{1u}^{A1}$
	244	
7849		$^3A_{2g} \rightarrow {}^3E_g + 3E_{1u}^{A1}$
11236		$^3A_{2g} \rightarrow {}^3A_{2g}$
	160	
11396		$^3A_{2g} \rightarrow {}^3A_{2g} + 1(E_{1u}^{B} + A_{2u}^{B})$
	165	
11561		$^3A_{2g} \rightarrow {}^3A_{2g} + 2(E_{1u}^{B} + A_{2u}^{B})$
	176	
11737		$^3A_{2g} \rightarrow {}^3A_{2g} + 3(E_{1u}^{B} + A_{2u}^{B})$
	168	
11905		$^3A_{2g} \rightarrow {}^3A_{2g} + 4(E_{1u}^{B} + A_{2u}^{B})$
12077		$^3A_{2g} \rightarrow {}^3E_g$
	208	
12285		$^3A_{2g} \rightarrow {}^3E_g + A_{2u}^{A}$
	215	
12500		$^3A_{2g} \rightarrow {}^3E_g + 2A_{2u}^{A}$
12987		$^3A_{2g} \rightarrow {}^1E_g$
	300	
13287		$^3A_{2g} \rightarrow {}^1E_g + 1(E_{1u}^{A1} + A_{2u}^{B})$
	300	
13587		$^3A_{2g} \rightarrow {}^1E_g + 2(E_{1u}^{A1} + A_{2u}^{B})$
	302	
13889		$^3A_{2g} \rightarrow {}^1E_g + 3(E_{u1}^{A1} + A_{2u}^{B})$
17857		$^3A_{2g} \rightarrow {}^1A_{1g}\,(^1T_{2g}, {}^1D)$
19231		$^3A_{2g} \rightarrow {}^1A_{1g}$
21834		$^3A_{2g} \rightarrow {}^3A_{2g}, {}^3E_g(^3T_{1g})$
23585		$^3A_{2g} \rightarrow {}^1A_{2g}\,(^1T_{1g})$
24038		$^3A_{2g} \rightarrow {}^1E_g\,(^1T_{1g})$
25707		$^3A_{2g} \rightarrow {}^1E_{1g}\,(^1E_{1g})$
	335	
26042		$^3A_{2g} \rightarrow {}^1A_{1g}\,(^1T_{2g}, {}^1G)$
	191	
26233		$^3A_{2g} \rightarrow A_{1g} + A_{2u}^{A}$
	222	
26455		$^3A_{2g} \rightarrow A_{2g} + 2A_{2u}^{A}$

TABLE I—*continued*

E, cm^{-1}	ΔE	Assignment
		$E\|\|xy$
6667		$^3A_{2g} \rightarrow {}^3A_{1g}$
7143		$^3A_{2g} \rightarrow {}^3E_g$
	237	
7380		$^3A_{2g} \rightarrow {}^3E_g + E_{1u}^{A1}$
	225	
7605		$^3A_{2g} \rightarrow {}^3E_g + 2E_{1u}^{A1}$
	244	
7819		$^3A_{2g} \rightarrow {}^3E_g + 3E_{1u}^{A1}$
11173		$^3A_{2g} \rightarrow {}^3A_{2g}$
11429		$^3A_{2g} \rightarrow {}^3A_{2g} + 2E_{1u}^{A2}$
	198	
11628		$^3A_{2g} \rightarrow {}^3A_{2g} + 3E_{1u}^{A2}$
12077		$^3A_{2g} \rightarrow {}^3E_g$
	193	
12270		$^3A_{2g} \rightarrow {}^3E_g + E_{1u}^{A2}$
12953		$^3A_{2g} \rightarrow {}^1E_g$
	310	
13263		$^3A_{2g} \rightarrow {}^1E_g + 1(E_{1u}^{A1} + A_{2u}^{B})$
	315	
13578		$^3A_{2g} \rightarrow {}^1E_g + 2(E_{1u}^{A1} + A_{2u}^{B})$
	311	
13889		$^3A_{2g} \rightarrow {}^1E_g + 3(E_{1u}^{A1} + A_{2u}^{B})$
17857		$^3A_{2g} \rightarrow {}^1A_{1g}\,(^1T_{2g}, {}^1D)$
19048		$^3A_{2g} \rightarrow {}^1A_{1g}$
19417		$^3A_{2g} \rightarrow {}^1A_{1g} + ?$
21834		$^3A_{2g} \rightarrow {}^3E_g, {}^3A_{2g}$
24096		$^3A_{2g} \rightarrow {}^1E_g\,(^1T_{1g})$
26247		$^3A_{2g} \rightarrow {}^1A_{1g}\,(^1T_{2g}, {}^1D)$

[a] All first components are pseudo-origins (the Ni atom in these compounds sits on a center of inversion) and should have the upper state written as the sum of the electronic state plus the allowing phonon mode. In certain cases, however, there is only one component negating the possibility of deciding which vibrational frequency is important. Therefore, for the sake of consistency we have chosen to write all first components as if they were origins keeping in mind that they are pseudo-origins.

[b] Superscript *A* indicates vibration is a molecular mode and *B* indicates a lattice mode.

TABLE II

THE ABSORPTION SPECTRUM OF $[(CH_3)_4N]NiCl_3$ AT 5°K

E, cm^{-1}	ΔE	Assignment
		$E\|\|z$
5613		$^3A_{2g} \rightarrow {}^3A_{1g} + 2(A_{2u}^B + E_{2g}^B)$
	109	
5722		$^3A_{2g} \rightarrow {}^3A_{1g} + 3(A_{2u}^B + E_{2g}^B)$
	100	
5822		$^3A_{2g} \rightarrow {}^3A_{1g} + 4(A_{2u}^B + E_{2g}^B)$
	103	
5926		$^3A_{2g} \rightarrow {}^3A_{1g} + 5(A_{2u}^B + E_{2g}^B)$
	113	
6006		$^3A_{2g} \rightarrow {}^3A_{1g} + 5(A_{2u}^B + E_{2g}^B) + E_{1u}^B$
6039		$^3A_{2g} \rightarrow {}^3A_{1g} + 6(A_{2u}^B + E_{2g}^B)$
6410		$^3A_{2g} \rightarrow {}^3A_{1g} + ?$
6887		$^3A_{2g} \rightarrow {}^3A_{1g} + ?$
	106	
6993		$^3A_{2g} \rightarrow {}^3A_{1g} + ?$
7220		$^3A_{2g} \rightarrow {}^3E_g + 1E_{1u}^{A1}$
	243	
7463		$^3A_{2g} \rightarrow {}^3E_g + 2E_{1u}^{A1}$
	259	
7722		$^3A_{2g} \rightarrow {}^3E_g + 3E_{1u}^{A1}$
	246	
7968		$^3A_{2g} \rightarrow {}^3E_g + 4E_{1u}^{A1}$
8621		$^3A_{2g} \rightarrow ?$
11364		$^3A_{2g} \rightarrow {}^3E_g$
12870		$^3A_{2g} \rightarrow {}^1E_g$
	323	
13193		$^3A_{2g} \rightarrow {}^1E_g + 1(E_{1u}^{A1} + A_{2u}^B)$
	321	
13514		$^3A_{2g} \rightarrow {}^1E_g + 2(E_{2u}^{A1} + A_{2u}^B)$
18957		$^3A_{2g} \rightarrow {}^1A_{1g}$
19685		$^3A_{2g} \rightarrow ?$
21008		$^3A_{2g} \rightarrow {}^3A_{2g}$
21834		$^3A_{2g} \rightarrow {}^1A_{2g}\,(^1T_{1g})$
23529		$^3A_{2g} \rightarrow {}^1E_g\,(^1T_{1g})$
25974		$^3A_{2g} \rightarrow {}^1E_g\,(^1E_g)$

TABLE II—*continued*

E, cm^{-1}	ΔE		Assignment
		$E\|\|xy$	
5394			$^3A_{2g} \rightarrow {}^3A_{1g}$
	111		
5495			$^3A_{2g} \rightarrow {}^3A_{1g} + 1(A_{2u}^B + E_{2g}^B)$
	107		
5602			$^3A_{2g} \rightarrow {}^3A_{1g} + 2(A_{2u}^B + E_{2g}^B)$
5674	120		$^3A_{2g} \rightarrow {}^3A_{1g} + 2(A_{2u}^B + E_{2g}^B) + E_{1u}^B$
5722		133	$^3A_{2g} \rightarrow {}^3A_{1g} + 3(A_{2u}^B + E_{2g}^B)$
5807	143		$^3A_{2g} \rightarrow {}^3A_{1g} + 3(A_{2u}^B + E_{2g}^B) + E_{1u}^B$
5865		117	$^3A_{2g} \rightarrow {}^3A_{1g} + 4(A_{2u}^B + E_{2g}^B)$
5924	123		$^3A_{2g} \rightarrow {}^3A_{1g} + 4(A_{2u}^B + E_{2g}^B) + E_{1u}^B$
5988		109	$^3A_{2g} \rightarrow {}^3A_{1g} + 5(A_{2u}^B + E_{2g}^B)$
6033			$^3A_{2g} \rightarrow {}^3A_{1g} + 5(A_{2u}^B + E_{2g}^B) + E_{1u}^B$
6410			$^3A_{2g} \rightarrow$?
6873			$^3A_{2g} \rightarrow {}^3E_g$
	270		
7143			$^3A_{2g} \rightarrow {}^3E_g + E_{1u}^{A1}$
	237		
7380			$^3A_{2g} \rightarrow {}^3E_g + 2E_{1u}^{A1}$
	254		
7634			$^3A_{2g} \rightarrow {}^3E_g + 3E_{1u}^{A1}$
	240		
7874			$^3A_{2g} \rightarrow {}^3E_g + 4E_{1u}^{A1}$
8547			$^3A_{2g} \rightarrow$?
10638			$^3A_{2g} \rightarrow {}^3A_{2g}$
11561			$^3A_{2g} \rightarrow {}^3E_g + E_{1u}^{A1}$
12821			$^3A_{2g} \rightarrow {}^1E_g$
	302		
13123			$^3A_{2g} \rightarrow {}^1E_g + 1(E_{1u}^{A1} + A_{2u}^B)$
	300		
13423			$^3A_{2g} \rightarrow {}^1E_g + 2(E_{1u}^{A1} + A_{2u}^B)$
17699			$^3A_{2g} \rightarrow {}^1E_g, {}^1A_{2g}\ (^1T_{1g})$
18692			$^3A_{2g} \rightarrow {}^1A_{1g}$
19608			$^3A_{2g} \rightarrow {}^3E_g\ (^3T_{2g}) + {}^1E_g\ (^1E_g)$
21390			$^3A_{2g} \rightarrow {}^3E_g$
24096			$^3A_{2g} \rightarrow {}^1E_g\ (^1T_{1g})$
25641			$^3A_{2g} \rightarrow {}^1E_g$
28571			$^3A_{2g} \rightarrow {}^1E_g\ (^1T_{2g}, {}^1G)$

TABLE III

THE ABSORPTION SPECTRUM OF $CsNiCl_3$ AT 5°K

E, cm^{-1}	ΔE	Assignment
		$E\|\|z$
6667		$^3A_{2g} \rightarrow {}^3A_{1g}$
7299		$^3A_{2g} \rightarrow {}^3E_g$
	248	
7547		$^3A_{2g} \rightarrow {}^3E_g + 1E_{1u}^{A1}$
	253	
7800		$^3A_{2g} \rightarrow {}^3E_g + 2E_{1u}^{A1}$
	271	
8071		$^3A_{2g} \rightarrow {}^3E_g + 3E_{1u}^{A1}$
10336		$^3A_{2g} \rightarrow {}^3A_{2g}$
	213	
10549		$^3A_{2g} \rightarrow {}^2A_{2g} + A_{2u}^{A}$
	262	
10811		$^3A_{2g} \rightarrow {}^3A_{2g} + A_{2u}^{A} + E_{1u}^{A1}$
10949		$^3A_{2g} \rightarrow {}^3E_g$
	232	
11173		$^3A_{2g} \rightarrow {}^3E_g + 1(E_{1u}^{A2} + A_{2u}^{B})$
	229	
11402		$^3A_{2g} \rightarrow {}^3E_g + 2(E_{1u}^{A2} + A_{2u}^{B})$
	226	
11628		$^3A_{2g} \rightarrow {}^3E_g + 3(E_{1u}^{A2} + A_{2u}^{B})$
	220	
11848		$^3A_{2g} \rightarrow {}^3E_g + 4(E_{1u}^{A2} + A_{1u}^{B})$
	229	
12077		$^3A_{2g} \rightarrow {}^3E_g + 5(E_{1u}^{A2} + A_{2u}^{B})$
	238	
12315		$^3A_{2g} \rightarrow {}^3E_g + 6(E_{1u}^{A2} + A_{2u}^{B})$
	216	
12531		$^3A_{2g} \rightarrow {}^3E_g + 7(E_{1u}^{A2} + A_{2u}^{B})$
12920		$^3A_{2g} \rightarrow {}^1E_{1g}$
	325	
13245		$^3A_{2g} \rightarrow {}^1E_{1g} + 1(E_{1u}^{A1} + A_{2u}^{B})$
	305	
13550		$^3A_{2g} \rightarrow {}^1E_{1g} + 2(E_{1u}^{A1} + A_{2u}^{B})$
	320	
13870		$^3A_{2g} \rightarrow {}^1E_g + 3(E_{1u}^{A1} + A_{2u}^{B})$
17857		$^3A_{2g} \rightarrow {}^1A_{1g}\,(^1T_{2g}, {}^1D)$
18939		$^3A_{2g} \rightarrow {}^1A_{1g}$
21978		$^3A_{2g} \rightarrow {}^3E_g\,(^3T_{2g})$
	274	
22252		$^3A_{2g} \rightarrow {}^3T_{2g} + 1(A_{2u}^{A} + E_{1u}^{B})$
	271	
22523		$^3A_{2g} \rightarrow {}^3T_{2g} + 2(A_{2u}^{A} + E_{1u}^{B})$
	282	
22805		$^3A_{2g} \rightarrow {}^3T_{2g} + 3(A_{2u}^{A} + E_{1u}^{B})$
23697		$^3A_{2g} \rightarrow {}^1A_{2g}$
25773		$^3A_{2g} \rightarrow {}^1E_{1g}\,(^1E_g)$, $^1A_{2g}\,(^1T_{2g}, {}^1G)$
25974		$^3A_{2g} \rightarrow {}^1E_g\,(^1T_{2g}, {}^1G)$

TABLE III—*continued*

E, cm^{-1}	ΔE	Assignment
		$E\|\|xy$
6645		$^3A_{2g} \rightarrow {}^3A_{1g}$
	252	
6897		$^3A_{2g} \rightarrow {}^3A_{1g} + 1E_{1u}^{A1}$
	271	
7168		$^3A_{2g} \rightarrow {}^3A_{1g} + 2E_{1u}^{A1}$
	261	
7429		$^3A_{2g} \rightarrow {}^3A_{1g} + 3E_{1u}^{A1}$
	251	
7680		$^3A_{2g} \rightarrow {}^3A_{1g} + 4E_{1u}^{A1}$
	257	
7937		$^3A_{2g} \rightarrow {}^3A_{1g} + 5E_{1u}^{A1}$
11223		$^3A_{2g} \rightarrow {}^3E_g$
	208	
11344		$^3A_{2g} \rightarrow {}^3E_g + (E_{1u}^{B} + A_{2u}^{B})$
11431		$^3A_{2g} \rightarrow {}^3E_g + 1(E_{1u}^{A2} + A_{2u}^{B})$
	197	
11570		$^3A_{2g} \rightarrow {}^3E_g + (E_{1u}^{A2} + A_{2u}^{B} + E_{1u}^{B} + A_{2u}^{B})$
11628		$^3A_{2g} \rightarrow {}^3E_g + 2(E_{1u}^{A2} + A_{2u}^{B})$
	212	
11840		$^3A_{2g} \rightarrow {}^3E_g + 3(E_{1u}^{A2} + A_{2u}^{B})$
	215	
12055		$^3A_{2g} \rightarrow {}^3E_g + 4(E_{1u}^{A2} + A_{2u}^{B})$
	230	
12285		$^3A_{2g} \rightarrow {}^3E_g + 5(E_{1u}^{A2} + A_{2u}^{B})$
	231	
12516		$^3A_{2g} \rightarrow {}^3E_g + 6(E_{1u}^{A2} + A_{2u}^{B})$
12719		$\Gamma_1 \rightarrow \Gamma_5$
12920		$^3A_{2g} \rightarrow {}^1E_g$
	325	
13245		$^3A_{2g} \rightarrow {}^1E_g + 1(E_{1u}^{A1} + A_{2u}^{B})$
	305	
13550		$^3A_{2g} \rightarrow {}^1E_g + 2(E_{1u}^{A1} + A_{2u}^{B})$
	320	
13870		$^3A_{2g} \rightarrow {}^1E_g + 3(E_{1u}^{A1} + A_{2u}^{B})$
18248		$^3A_{2g} \rightarrow {}^3E_g\,(^1T_{2g}, {}^1D)$
	151	
18399		$^3A_{2g} \rightarrow {}^1E_g + ?$
	154	
18553		$^3A_{2g} \rightarrow {}^1E_g + ?$
18939		$^3A_{2g} \rightarrow {}^1A_{1g}$
19305		$^3A_{2g} \rightarrow {}^1A_{1g} + ?$
21692		$^3A_{2g} \rightarrow {}^3A_{2g}\,(^3T_{1g})$
24067		$^3A_{2g} \rightarrow {}^1E_g\,(^1T_{1g})$
26042		$^3A_{2g} \rightarrow {}^1E_g\,(^1E_{1g}), {}^1A_{1g}\,(^1T_{1g})$

TABLE IV

THE ABSORPTION SPECTRUM OF $RbNiCl_3$ AT 5°K

E, cm^{-1}	ΔE	Assignment
		$E\|\|z$
6849		$^3A_{2g} \rightarrow {}^3A_{1g}$
7246		$^3A_{2g} \rightarrow {}^3E_g$
	217	
7463		$^3A_{2g} \rightarrow {}^3E_g + 1(E_{1u}^{A2} + A_{2u}^{B})$
	229	
7692		$^3A_{2g} \rightarrow {}^3E_g + 2(E_{1u}^{A2} + A_{2u}^{B})$
11331		$^3A_{2g} \rightarrow {}^3A_{2g}$
	163	
11494		$^3A_{2g} \rightarrow {}^3A_{2g} + (A_{2u}^{A} - A_{2u}^{B})$
	161	
11655		$^3A_{2g} \rightarrow {}^3A_{2g} + 2(A_{2u}^{A} - A_{2u}^{B})$
	158	
11813		$^3A_{2g} \rightarrow {}^3A_{2g} + 3(A_{2u}^{A} - A_{2u}^{B})$
	221	
12034		$^3A_{2g} \rightarrow {}^3E_g$
	243	
12277		$^3A_{2g} \rightarrow {}^3E_g + 1(E_{1u}^{A2} + A_{2u}^{B})$
	223	
12500		$^3A_{2g} \rightarrow {}^3E_g + 2(E_{1u}^{A2} + A_{2u}^{B})$
	239	
12739		$^3A_{2g} \rightarrow {}^3E_g + 3(E_{1u}^{A2} + A_{2u}^{B})$
13012		$^3A_{2g} \rightarrow {}^1E_g$
	321	
13333		$^3A_{2g} \rightarrow {}^1E_g + 1(E_{1u}^{A1} + A_{2u}^{B})$
	310	
13643		$^3A_{2g} \rightarrow {}^1E_g + 2(E_{1u}^{A1} + A_{2u}^{B})$
	304	
13947		$^3A_{2g} \rightarrow {}^1E_g \quad 3(E_{1u}^{A1} + A_{2u}^{B})$
	298	
14245		$^3A_{2g} \rightarrow {}^1E_g + 4(E_{1u}^{A1} + A_{2u}^{B})$
22222		$^3A_{2g} \rightarrow {}^3E_g\,(^3T_{1g})$
23810		$^3A_{2g} \rightarrow {}^1A_{2g}\,(^1T_{1g})$
26178		$^3A_{2g} \rightarrow {}^1E_g\,(^1E_g), {}^1E_{1g}\,(^1T_{1g})$

TABLE IV—*continued*

E, cm^{-1}	ΔE	Assignment
		$E\|\|xy$
6849		$^3A_{2g} \rightarrow {}^3A_{1g}$
7042	243	$^3A_{2g} \rightarrow$?
7092	284	$^3A_{2g} \rightarrow {}^3A_{1g} + 1(E_{1u}^{A2} + E_{2g}^{B})$
7231	234	$^3A_{2g} \rightarrow {}^3E_g$
7326		$^3A_{2g} \rightarrow {}^3A_{1g} + 2(E_{1u}^{A2} + E_{2g}^{B})$
	244	
7570		$^3A_{2g} \rightarrow {}^3A_{1g} + 3(E_{1u}^{A2} + E_{2g}^{B})$
	243	
7813		$^3A_{2g} \rightarrow {}^3A_{1g} + 4(E_{1u}^{A2} + E_{2g}^{B})$
11312		$^3A_{2g} \rightarrow {}^3A_{2g}$
	195	
11507		$^3A_{2g} \rightarrow {}^3A_{2g} + E_{1u}^{A2}$
	189	
11696		$^3A_{2g} \rightarrow {}^3A_{2g} + 2E_{1u}^{A2}$
	$374 = 2 \times 187$	
12070		$^3A_{2g} \rightarrow {}^3A_{2g} + 4E_{1u}^{A2}$
	200	
12270		$^3A_{2g} \rightarrow {}^3A_{2g} + 5E_{1u}^{A2}$
	199	
12469		$^3A_{2g} \rightarrow {}^3A_{2g} + 6E_{1u}^{A2}$
12821		$\Gamma_1 \rightarrow \Gamma_5$
	208	
13029		$^3A_{2g} \rightarrow {}^1E_g$
	304	
13333		$^3A_{2g} \rightarrow {}^1E_g + 1(E_{1u}^{A1} + A_{2u}^{B})$
	300	
13633		$^3A_{2g} \rightarrow {}^1E_g + 2(E_{1u}^{A1} + A_{2u}^{B})$
	304	
13937		$^3A_{2g} \rightarrow {}^1E_g + 3(E_{1u}^{A1} + A_{2u}^{B})$
19048		$^3A_{2g} \rightarrow {}^1A_{1g}$
21834		$^3A_{2g} \rightarrow {}^3A_{2g}\,(^3T_{1g})$
24038		$^3A_{2g} \rightarrow {}^1E_g\,(^1T_{1g})$
26247		$^3A_{2g} \rightarrow {}^1E_g\,(^1E_g) + {}^1A_{1g}\,(^1T_{2g})$

TABLE V

THE ABSORPTION SPECTRUM OF $CsNiBr_3$ AT 5°K

E, cm^{-1}	ΔE	Assignment
		$E\|\|z$
6369		$^3A_{2g} \rightarrow {}^3A_{1g}$
6826		$^3A_{2g} \rightarrow {}^3E_g$
6897		$^3A_{2g} \rightarrow {}^3E_g + E^B_{1u}$
	155	
7052		$^3A_{2g} \rightarrow {}^3E_g + E^B_{1u} + 1E^{A2}_{1u}$
	168	
7220		$^3A_{2g} \rightarrow {}^3E_g + E^B_{1u} + 2E^{A2}_{1u}$
	171	
7391		$^3A_{2g} \rightarrow {}^3E_g + E^B_{1u} + 3E^{A2}_{1u}$
	173	
7564		$^3A_{2g} \rightarrow {}^3E_g + E^B_{1u} + 4E^{A2}_{1u}$
	188	
7752		$^3A_{2g} \rightarrow {}^3E_g + E^B_{1u} + 5E^{A2}_{1u}$
10515		$^3A_{2g} \rightarrow {}^3A_{2g} + A_{2u}$
	101	
10616		$^3A_{2g} \rightarrow {}^3A_{2g} + ?$
	254	
10870		$^3A_{2g} \rightarrow {}^3A_{2g} + ?$
	168	
11038		$^3A_{2g} \rightarrow {}^3A_{2g} + ?$
	198	
11236		$^3A_{2g} \rightarrow {}^3E_g$
	258	
11494		$^3A_{2g} \rightarrow {}^3E_g + E^{A1}_{1u}$
	257	
11751		$^3A_{2g} \rightarrow {}^3E_g + 2E^{A2}_{1u}$
	225	
11976		$^3A_{2g} \rightarrow {}^1E_g$
	182	
12158		$^3A_{2g} \rightarrow {}^1E_g + 1E^{A2}_{1u}$
	188	
12346		$^3A_{2g} \rightarrow {}^1E_g + 2E^{A2}_{1u}$
	185	
12531		$^3A_{2g} \rightarrow {}^1E_g + 3E^{A2}_{1u}$
16529		$^3A_{2g} \rightarrow {}^1E_g + {}^1A_{2g}$
16667		$^3A_{2g} \rightarrow {}^1E_g + {}^1A_{2g} + ?$
16978		$^3A_{2g} \rightarrow {}^1E_g + {}^1A_{2g} + ?$
	263	
17241		$^3A_{2g} \rightarrow {}^1E_g + {}^1A_{2g} + ?$
17606		$^3A_{2g} \rightarrow {}^1A_{1g}$
20408		$^3A_{2g} \rightarrow {}^3A_{2g}, {}^3E_g$

TABLE V—*continued*

E, cm^{-1}	ΔE	Assignment
		$E\|\|xy$
6369		$^3A_{2g} \rightarrow {}^3A_{1g}$
6821		$^3A_{2g} \rightarrow {}^3E_g$
	167	
6988		$^3A_{2g} \rightarrow {}^3E_g + E^{A2}_{1u}$
	$332 = 2 \times 166$	
7220		$^3A_{2g} \rightarrow {}^3E_g + 3E^{A2}_{1u}$
	171	
7391		$^3A_{2g} \rightarrow {}^3E_g + 4E^{A2}_{1u}$
10309		$^3A_{2g} \rightarrow {}^3A_{2g}$
11614		$^3A_{2g} \rightarrow {}^3E_g$
	165	
11779		$\Gamma_1 \rightarrow \Gamma_5$
	197	
11976		$^3A_{2g} \rightarrow {}^1E_g$
	219	
12195		$^3A_{2g} \rightarrow {}^1E_g + A^A_{2u}$
	212	
12407		$^3A_{2g} \rightarrow {}^1E_g + 2A^A_{2u}$
	172	
12579		$^3A_{2g} \rightarrow {}^1E_g + 2A^A_{2u} + E^{A2}_{2u}$
	209	
12788		$^3A_{2g} \rightarrow {}^1E_g + 3A^A_{2u} + E^{A2}_{2u}$
13500		$^3A_{2g} \rightarrow {}^3E_g\,(T_{2g}) + {}^3E_g\,(T_{2g})$
16529		$^3A_{2g} \rightarrow {}^1E_g + {}^1A_{2g}\,({}^1T_{2g}, {}^1D)$
17699		$^3A_{2g} \rightarrow {}^1A_{1g}$
20408		$^3A_{2g} \rightarrow {}^3A_{2g} + {}^3E_g$
21834		$^3A_{2g} \rightarrow {}^1A_{2g}, {}^1E_g\,({}^1T_{1g})$
23669		$^3A_{2g} \rightarrow {}^1E_g\,({}^1E_g)$

TABLE VI

CALCULATED ENERGIES FOR TRANSITIONS IN M^INiX_3 IN cm^{-1} (*21*)

	$Cs(Mg,Ni)Cl_3$ [a]	$[(CH_3)_4N]NiCl_3$ [b]	$CsNiCl_3$ [c]	$RbNiCl_3$ [d]	$CsNiBr_3$ [e]
$^3A_{2g} \rightarrow {}^3T_{2g}$	7053	6052	6855	7288	6535
$^3A_{2g} \rightarrow {}^3T_{1g}$	11811	10549	11315	12139	10840
$^3A_{2g} \rightarrow {}^1E_g$	13826	13341	13661	13857	11860
$^3A_{2g} \rightarrow {}^1T_{2g}$	19039	18199	18816	19342	18786
$^3A_{2g} \rightarrow {}^1A_{1g}$	20554	20170	20442	20587	19600
$^3A_{2g} \rightarrow {}^3T_{1g}$	22565	20674	22297	22880	20205
$^3A_{2g} \rightarrow {}^1T_{1g}$	23585	22641	23386	23800	21630
$^3A_{2g} \rightarrow {}^1E_g$	28603	27279	28219	29044	26820

[a] $D_q = -700$, $F_2 = 1300$, $F_4 = 90$, $\lambda = -225$.
[b] $D_q = -600$, $F_2 = 1300$, $F_4 = 100$, $\lambda = -225$.
[c] $D_q = -680$, $F_2 = 1300$, $F_4 = 90$, $\lambda = -225$.
[d] $D_q = -725$, $F_2 = 1300$, $F_4 = 90$, $\lambda = -175$.
[e] $D_q = -650$, $F_2 = 1200$, $F_4 = 85$, $\lambda = -175$.

TABLE VII

OSCILLATOR STRENGTHS FOR SELECTED TRANSITION IN M^INiX_3

Compound	Polarization	Transition	$f \times 10^5$ (300°K)	$f \times 10^5$ (77°K)	$f \times 10^5$ (4°K)
$[(CH_3)_4N]NiCl_3$	$\perp$	$^3A_{2g} \rightarrow {}^3T_{2g}$	1.1	0.9	0.9
		$^3A_{2g} \rightarrow {}^3T_{1g}(F)$	1.5	1.3	1.2
		$^3A_{2g} \rightarrow {}^1E_g(D)$			.2
		$^3A_{2g} \rightarrow {}^1A_{1g}(G)$			.3
	$\parallel$	$^3A_{2g} \rightarrow {}^3T_{2g}$	1.6	1.5	1.4
		$^3A_{2g} \rightarrow {}^3T_{1g}(F)$	2.4	2.1	2.0
		$^3A_{2g} \rightarrow {}^1E_g(D)$			0.2
		$^3A_{2g} \rightarrow {}^1A_{1g}(G)$			0.6
$CsNiCl_3$	$\perp$	$^3A_{2g} \rightarrow {}^3T_{2g}$	1.8	1.1	1.4
		$^3A_{2g} \rightarrow {}^3T_{1g}(F)$	4.7	1.8	1.8
		$^3A_{2g} \rightarrow {}^1E_g(D)$		0.2	0.4
		$^3A_{2g} \rightarrow {}^1A_{1g}(G)$	1.1	1.7	2.5
	$\parallel$	$^3A_{2g} \rightarrow {}^3T_{2g}$	4.1	1.9	2.0
		$^3A_{2g} \rightarrow {}^3T_{1g}(F)$	6.4	2.9	3.0
		$^3A_{2g} \rightarrow {}^1E_g(D)$		0.4	0.6
		$^3A_{2g} \rightarrow {}^1A_{1g}(G)$	0.4	0.7	0.8
$RbNiCl_3$	$\perp$	$^3A_{2g} \rightarrow {}^3T_{2g}$	1.8	1.5	1.5
		$^3A_{2g} \rightarrow {}^3T_{1g}(F)$	5.5	2.7	2.2
		$^3A_{2g} \rightarrow {}^1E_g(D)$			0.3
		$^3A_{2g} \rightarrow {}^1A_{1g}(G)$	1.2	2.2	2.5
	$\parallel$	$^3A_{2g} \rightarrow {}^3T_{2g}$	4.2	2.5	2.1
		$^3A_{2g} \rightarrow {}^3T_{1g}(G)$	6.0	3.3	2.6
		$^3A_{2g} \rightarrow {}^1E_g(D)$			0.5
		$^3A_{2g} \rightarrow {}^1A_{1g}(G)$	0.9	0.9	1.0
$CsNiBr_3$	$\perp$	$^3A_{2g} \rightarrow {}^3T_{2g}$	3.0	1.9	1.8
		$^3A_{2g} \rightarrow {}^3T_{1g}(F)$	8.1	4.4	5.4
		$^3A_{2g} \rightarrow {}^1E_g(D)$			1.4
		$^3A_{2g} \rightarrow {}^1A_{1g}(G)$	3.7	5.4	8.5
	$\parallel$	$^3A_{2g} \rightarrow {}^3T_{2g}$	6.9	2.4	2.8
		$^3A_{2g} \rightarrow {}^3T_{1g}(F)$	11.7	5.2	4.8
		$^3A_{2g} \rightarrow {}^1E_g(D)$			0.7
		$^3A_{2g} \rightarrow {}^1A_{1g}(G)$	1.9	3.6	4.8

for the transitions in the various compounds. Table VII contains a tabulation of oscillator strengths vs temperature for the pure $M^{I}NiCl_3$ and $CsNiBr_3$.

Measurements of the axial spectra agree in all cases with the $\sigma(x,y)$ spectra, indicating all bands are allowed by an electric dipole process.

Discussion

General Features. Ni^{2+} is a d^8 system. In octahedral symmetry its electronic ground state is $^3A_{2g}$. Transitions are possible to three spin triplets. In order of increasing energy these are $^3T_{2g}$, $^3T_{1g}(F)$, and $^3T_{1g}(P)$. Transitions are also possible to a variety of spin singlets. The order in which these transitions occur is somewhat dependent upon the strength of the crystal field. In D_{3d} symmetry the following correlations exist: $A_{1g} \rightarrow A_{1g}$, $A_{2g} \rightarrow A_{2g}$, $E_g \rightarrow E_g$, $T_{1g} \rightarrow E_g + A_{2g}$ and $T_{2g} \rightarrow E_g + A_{1g}$.

Transition energies derived from the matrices of Liehr and Ballhausen (*22*) for 0_h $d^{2,8}$ ions, Table VI, account for the general features of the spectra recorded in this work. An apparent trend in D_q, $[(CH_3)_4N]NiCl_3 < CsNiCl_3 < RbNiCl_3$, exists as a function of decreasing cation size. While too much emphasis should not be placed upon this trend due to the difficulty of assigning a reasonable center of gravity of of envelopes (occasioned by the complexity of the data) it would appear that this is a genuine effect and is most likely related to increasing intrachain compression rather than transverse next nearest neighbor interaction.

Utilizing the polarization behavior and taking into account the available phonon modes, the ordering of the transitions in D_{3d} symmetry can be ascertained. This is shown in Tables I–V. In all cases for the lowest energy manifold we find two pseudo-origins present. The least energetic of these is the $^3A_{2g} \rightarrow {}^3A_{2g}(^3T_{2g})$ transition. This trigonal splitting ranges from $\sim$1600 cm^{-1} in $[(CH_3)_4N]NiCl_3$ to $\sim$400 cm^{-1} in $RbNiCl_3$.

The next highest manifold, in the 11 000 cm^{-1} region, contains three origins rather than the two predicted for a D_{3d} split $T_{1g}(F)$ state. One of these origins is of A_{2g} symmetry while the other two are of E_g symmetry. Since it is known that the $^3A_{2g} \rightarrow {}^1E_g$ transition lies in this region we may account for the two lowest energy origins by assigning them to components of the $^3T_{1g}(F)$ state while the higher E_g state is assigned as the $^3A_{2g} \rightarrow {}^1E_g$ transition. This assignment is based both upon the results of the calculations, Table VI, and the fact that the band shape of the highest energy origin is consistent with this assignment.

Turning our attention to $Cs(Mg,Ni)Cl_3$ and $[(CH_3)_4N]NiCl_3$ we note maxima at $\sim$18 000 cm^{-1} and $\sim$19 000 cm^{-1} in both compounds. The small intensity of these bands is indicative of transitions of a spin forbidden nature. Based upon our calculations we assign these bands to transitions of $^3A_{2g} \rightarrow {}^1T_{2g}$ and $^1A_{1g}$ parentage. The relatively sharp maximum occurring at $\sim$19 600 cm^{-1} in the spectrum of $[(CH_3)_4N]NiCl_3$ will be discussed later. By analogy the excitations in the 18 000–20 000 cm^{-1} range of $CsNiCl_3$ and $RbNiCl_3$ and 16 000–18 000 cm^{-1} region in $CsNiBr_3$, while anomalously intense, must be related to the $^3A_{2g} \rightarrow {}^1T_{2g}$ and $^1A_{1g}$ transitions.

The next highest energy band in all spectra is the $^3A_{2g} \rightarrow {}^3T_{1g}(P)$ transition. Beyond this maximum are further maxima which may be assigned to various high energy spin forbidden transitions. These assignments are tabulated in Tables I–V.

Intensity of $^3A_{2g} \rightarrow {}^1X$. Upon inspection of Table VII and Figs. 1–15 several outstanding features are apparent: (1) All the spin forbidden bands in $CsNiCl_3$, $RbNiCl_3$, and $CsNiBr_3$ are anomalously intense both with respect to $Cs(Mg,Ni)Cl_3$ and $[(CH_3)_4N]NiCl_3$ and to more common magnetically dilute Ni^{2+} compounds. (2) For the spin forbidden transitions, e.g., $^3A_{2g} \rightarrow {}^1A_{1g}$ in $CsNiCl_3$, $RbNiCl_3$, and $CsNiBr_3$ the $\perp Z$ polarization is always the most intense polarization. This is not necessarily true for the spin allowed transitions. (3) There is no significant difference in the intensities of spin forbidden transitions in going from the Rb^+ to the Cs^+ salt, i.e., increasing the interchain distances. (4) Replacement of chlorine with bromine in these systems enhances the intensity of the $^3A_{2g} \rightarrow {}^1X$ transitions. It also enhances the intensity of the $^3A_{2g} \rightarrow {}^3Y$ transitions. (4) There is a marked increase in the intensity of the $^3A_{2g} \rightarrow {}^1X$ transitions in going from 300°K to 80°K. There is also a large increase in intensity when the temperature is reduced from 80°K to 4°K. This effect *appears* to be greater for the bromide than for the chlorides. (6) There is no significant shift of the absorption maxima of the $^3A_{2g} \rightarrow {}^1X$ transitions as the temperature decreases.

From the above we can conclude several things: (1) The major contribution to the intensity of the ${}^3A_{2g} \rightarrow {}^1X$ transition arises from a cooperative phenomenon. (2) The dominant intensity giving mechanism arises from an intrachain rather than an interchain process. This is evidenced by the facts that the more intense polarization is perpendicular to the chain axis and that there is no significant difference in the intensities of analogous ${}^3A_{2g} \rightarrow {}^1X$ transitions in $CsNiCl_3$ and $RbNiCl_3$. (3) There is no discernible Ni–Ni bonding occurring else the chlorides which have shorter Ni–Ni distances than the bromide would exhibit more intense spin forbidden transitions than the bromide. (4) Ligand spin orbit coupling may be important in the exchange mechanism, however little can be said about this as while the spin forbidden transitions are more intense in the bromide than in the chlorides so are the spin allowed transitions. This suggests that covalency is at least in part responsible for the phenomenon.

Lohr and McClure (*23*) have suggested that analogous intensity enhancement, in magnetically concentrated Mn^{2+} systems, can occur via an exchange interaction between pairs of magnetically coupled ions. In the case where the interaction is pairwise the intensity of an absorption band is seen to vary but little above the Neel temperature. This is consistent with the idea that in pair interactions we are dealing with an exchange process which is dependent only upon a concerted two-ion transition in which spin deviation and electronic transition can occur simultaneously and are thus not dependent upon an antiferromagnetically ordered system. McPherson and Stucky (*20*) have suggested that it is the mechanism of Lohr and McClure which is operative in $CsNiCl_3$ and $RbNiCl_3$.

Druzhinin et al. (*24*) have taken a somewhat more sophisticated approach and have applied the two-spin cluster model of Oguchi (*25*) to antiferromagnetic $KNiF_3$. Their results, which fit the observed experimental behavior remarkably well, predict a major shift to higher energy of the maxima of the ${}^3A_{2g} \rightarrow {}^1X$ transitions near the Neel temperature. In addition the intensities of the various ${}^3A_{2g} \rightarrow {}^1X$ should be relatively insensitive to temperature changes above T_N.

Scrutiny of our experimental results leads us to the conclusion that the mechanism of Lohr and McClure is not adequate to explain the entire range of behavior observed here; unfortunately neither is that of Druzhinin et al. While it is logical to invoke an exchange mechanism of the Lohr–McClure type to explain the anomalous intensity of the ${}^3A_{2g} \rightarrow {}^1X$ at room temperature it would appear that the increase in intensity with decreasing temperature parallels somewhat the increase in numbers and chain length of antiferromagnetically coupled aggregates with decreasing temperature. Little more can be said in regard, however, without detailed measurements of T vs f throughout the entire temperature range.

Magnon Side Bands. In the $\perp$ polarization of the spectrum of $CsNiCl_3$ there is a well defined band located 200 cm^{-1} to lower energy than the ${}^1E_{1g}$ transition. It is also observed in the axial spectrum indicating that it is electric dipole in nature. It does not correlate with any available phonon mode. Upon dilution with $CsMgCl_3$ this maximum disappears entirely suggesting that it is not a single ion excitation. The presence of this maximum is best rationalized in terms of a magnon side band. For such concentrated-system-transitions to occur the product of the excited-state and the dipole moment of the exciting photon must transform as the totally symmetric representation of the space group. We may omit the ground-state in this product since it must transform as a totally symmetric state in the absence of electric and magnetic flux differences. Thus, as the (xy) dipole transforms as Γ_5, $\Gamma_5 \times \Gamma_{\text{excited-state}} \equiv \Gamma_1$.

The magnon states which result from the ${}^3A_{2g}$ ground state are Γ_1 and Γ_4 ($P6_3/mmc$) and those of the excitons associated with the ${}^1E_g$ excited state are Γ_5 and Γ_6. The states which describe magnon side bands may be formed from linear combinations of these magnon and exciton states. Since this crystal group does not contain the inversion operation, these linear combinations do not have to have negative parity; however, wave-vector conservation must be preserved. Thus the states which must be tested are of the form $(K, -K)$. If this state is $(\Gamma_5 K, \Gamma_1 - K)$ the total symmetry is Γ_5 and our absorption intensity product is Γ_1 giving an allowed transition which has state density at the Brillouin zone boundary points AHKLMP and vanishes elsewhere.

Of the three other concentrated systems of this study, $RbNiCl_3$ and $CsNiBr_3$ also exhibit an (xy) polarized electric dipole transition near the ${}^1E_g$ manifold which may be attributed to the same magnon side band state as that in $CsNiCl_3$ since these compounds are crystallographi-

cally isomorphous and magnetically similar. $[(CH_3)N]NiCl_3$ does not contain this sharp band due to its different crystal structure. Stucky has reported that $[(CH_3)N]NiCl_3$ belongs to the space group $P6_3/m$ which contains the inversion. operator. Recently, Gerstein et al. have shown that $TMANiCl_3$ is ferromagnetic. Thus there are restrictions upon the magnon side band state which do not allow it to exist, i.e., negative parity and wave vector conservation in a single sublattice system.

Double Ion Excitation. In the $\perp Z$ polarized absorption spectrum of $CsNiBr_3$, Fig. 15, there is a broad band at 13500 cm^{-1} which cannot be explained in terms of a single ion excitation. From an analysis of previously assigned transitions we suggest that this maximum conforms to an assignment as a simultaneous excitation of a coupled pair of Ni^{2+} ions i.e., $2(^3A_{2g} \rightarrow {}^3T_{2g})$. If we carefully scrutinize the temperature dependence of the band intensity we find that, within the limits of our data, it appears that the transition intensity is greater at 80°K than at 4° or 300°K. It we now turn our attention to $RbNiCl_3$, Fig. 13, we also find a broad maximum at an energy twice that of the $^3A_{2g} \rightarrow {}^3T_{2g}$ transition. Here the band is present at 80°K but not at 300° or 4°K. Such a temperature dependence cannot be explained via vibrational arguments but may be justified by considering the process of formation of coupled aggregates. At high temperatures there will be present exchange coupled pairs but virtually no antiferromagnetically coupled pairs. Here we do not see the double ion excitation, suggesting that exchange coupling is not important in the intensity-giving mechanism. As the temperature is decreased to 80°K the number of antiferromagnetically coupled pairs is increased and the intensity of the double ion excitation increases. With a further reduction in temperature the correlation length is increased and the double ion excitation appears to decrease in intensity in $CsNiBr_3$ and disappears in $RbNiCl_3$. This suggests that the transition is indeed dependent upon a pairwise interaction and that a long correlation length hampers the intensity giving mechanism. Why the effect should be more marked in $RbNiCl_3$ than in $CsNiBr_3$ is unclear at this time.

Turning our attention to the band at 19 600 cm^{-1} in $[(CH_3)_4N]NiCl_3$ we find that we have another case of a double ion excitation. Here the transition in question appears to be a $^3A_{2g} \rightarrow {}^3T_{2g} + {}^1E_g$ transition.

References

1. J. Milstein, J. Ackerman, S. L. Holt, and B. R. McGarvey, *Inorg. Chem.* **11**, 1178 (1972) and references therein; C. A. Kosky, B. R. McGarvey, and S. L. Holt, *J. Chem. Phys.* **56**, 5904 (1972); J. Jasinski and S. L. Holt, *Chem. Comm.* 1046 (1972).
2. S. L. Holt and A. Wold, *Inorg. Chem.* **6**, 1594 (1967); S. L. Holt and R. Dingle, *Acta Chem. Scand.* **22**, 1091 (1968); R. Dingle and S. L. Holt, *Acta Chem. Scand.* **22**, 2232 (1968); C. Simo and S. L. Holt, *Inorg. Chem.* **7**, 2655 (1968); E. M. Holt, S. L. Holt, and K. J. Watson, *J. Amer. Chem. Soc.* **92**, 2721 (1970).
3. B. Oral, S. L. Holt, and A. B. Denison, *J. Inorg. Nucl. Chem.* **34**, 1758 (1972) and references therein.
4. C. Simo and S. L. Holt, *J. Solid State Chem.* **4**, 76 (1972).
5. J. Ackerman, C. Fouassier, E. M. Holt, and S. L. Holt, *Inorg. Chem.* **11**, 3118 (1973).
6. R. Dingle, M. E. Lines, and S. L. Holt, *Phys. Rev. B* **187**, 643 (1969).
7. R. J. Birgeneau, R. Dingle, M. T. Hutchings, G. Shirane, and S. L. Holt, *Phys. Rev. Lett.* **26**, 718 (1971).
8. M. T. Hutchings, G. Shirane, R. J. Birgeneau, and S. L. Holt, *Phys. Rev. B* **5**, 1999 (1972).
9. N. Achiwa, *J. Phys. Soc. Japan* **27**, 561 (1969).
10. B. Morosin and E. J. Graeber, *Acta Cryst.* **23**, 766 (1967).
11. G. L. McPherson, T. J. Kistenmacher, and G. D. Stucky, *J. Chem. Phys.* **52**, 815 (1970).
12. For example see the summary by D. D. Sell, *J. Appl. Phys.* **39**, 1030 (1968).
13. S. J. Allen, R. Loudon, and P. L. Richards, *Phys. Rev. Lett.* **16**, 463 (1966).
14. P. A. Fleury, *Phys. Rev.* **180**, 591 (1969).
15. P. Martel, R. A. Cowley, and R. W. H. Stevenson, *J. Appl. Phys.* **39**, 1116 (1969).
16. R. W. Asmussen and H. Solig, *Z. Anorg. Allgen. Chem.* **283**, 3 (1956).
17. P. Day, *Proc. Chem. Soc.* **18** (1964).
18. W. E. Hatfield and T. S. Piper, *Inorg. Chem.* **3**, 841 (1964).
19. D. M. Goodgame, M. Goodgame, and M. J. Weeks, *J. Chem. Soc.* 5194 (1964).
20. G. L. McPherson and G. D. Stucky, *J. Chem. Phys.* **57**, 3780 (1972).
21. G. D. Stucky, *Acta Cryst.* **B24**, 330 (1968).
22. A. D. Liehr and C. J. Ballhausen, *Ann. Phys.* **6**, 134 (1959).
23. L. L. Lohr and D. S. McClure, *J. Chem. Phys.* **49**, 3516, (1968).
24. V. V. Druzhinin, R. V. Pisarev, and G. A. Karamysheva, *Sov. Phys. Solid State* **12**, 1789 (1971).
25. T. Oguchi, *Progr. Theor. Phys.* **13**, 148 (1955).